

# Accelerating the Design of Solar Thermal Fuel Materials through High Throughput Simulations

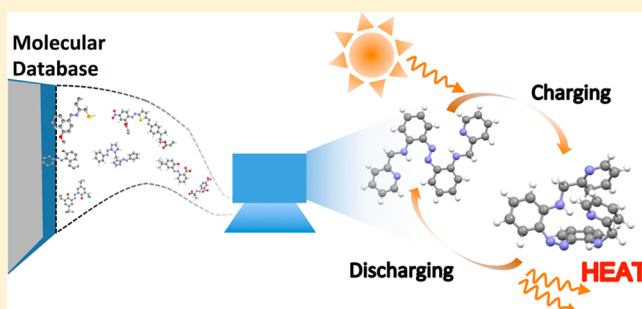
Yun Liu\* and Jeffrey C. Grossman\*

Department of Materials Science and Engineering, Massachusetts Institute of Technology, 77 Massachusetts Avenue, Cambridge, Massachusetts 02139, United States

## S Supporting Information

**ABSTRACT:** Solar thermal fuels (STF) store the energy of sunlight, which can then be released later in the form of heat, offering an emission-free and renewable solution for both solar energy conversion and storage. However, this approach is currently limited by the lack of low-cost materials with high energy density and high stability. In this Letter, we present an ab initio high-throughput computational approach to accelerate the design process and allow for searches over a broad class of materials. The high-throughput screening platform we have developed can run through large numbers of molecules composed of earth-abundant elements and identifies possible metastable structures of a given material. Corresponding isomerization enthalpies associated with the metastable structures are then computed. Using this high-throughput simulation approach, we have discovered molecular structures with high isomerization enthalpies that have the potential to be new candidates for high-energy density STF. We have also discovered physical principles to guide further STF materials design through structural analysis. More broadly, our results illustrate the potential of using high-throughput ab initio simulations to design materials that undergo targeted structural transitions.

**KEYWORDS:** Solar thermal fuel, high-throughput computation, ab initio simulation, photoisomerization



As a clean and renewable energy source, solar energy is a promising solution to the increasing energy demands of modern society. However, efficient and cost-effective conversion, storage, and distribution of solar energy remain a challenge. One approach to tackle this problem is to use a group of photoactive materials called solar thermal fuels (STF) to convert the sun's energy into stored chemical energy.<sup>1–4</sup> STF materials are capable of reconfiguring into higher energy metastable states using the energy of the absorbed photons. The amount of energy stored in the STF is approximately equal to the difference in enthalpy ( $\Delta H$ ) between the ground state and the metastable state of the material. The material can then remain in the metastable state for months or years, depending on the height of the energy barrier ( $E_a$ ) for the isomerization reaction from the metastable to the ground state, allowing storage and transportation of the STF in its “charged” state. Upon exposing the fuel to an external trigger such as heat, light, or a suitable catalyst, the STF will transform back to its ground state, releasing an amount of energy  $\Delta H$  in the form of heat. This energy can then be used in applications where direct heating is needed, and the fuel is then ready to be recharged by sunlight.

The STF approach, which in essence takes energy from the sun and puts it on a “chemical shelf” to be used when needed as heat-on-demand, has important advantages. It is an emission free closed-cycle system; the material charges “cold” by sunlight

and can be transported and distributed while charged without special thermal insulation; energy conversion from chemical energy to heat is theoretically 100% efficient, as there is no “wasted energy” in this process. However, as with many other renewable energy technologies, the challenge in making STF into a competitive alternative lies with the design of the material itself. The amount of light absorption, stored thermal energy  $\Delta H$ , and stability in the charged state  $E_a$ , all key performance metrics, are directly a function of the material choice.

A number of materials have been proposed as STF candidates over the past decades, including for example azobenzene,<sup>5,6</sup> norbornadiene,<sup>3</sup> fulvalene diruthenium,<sup>7,8</sup> and templating nanostructures with photoactive functional groups.<sup>9–11</sup> However, despite these advances to date the design of novel STF materials has occurred far too slowly in part due to the massive phase space of candidate materials and the serial nature of their exploration.

Here, we present an approach to design solar thermal fuels using high-throughput classical and ab initio simulations. The rapid advances in computing speed and algorithm development over the past several decades has led to the current “materials

**Received:** September 4, 2014

**Revised:** October 21, 2014

**Published:** November 5, 2014

genome" era of computational design,<sup>12</sup> wherein high-throughput ab initio simulation architectures enable automated materials discovery. This has proven highly successful in other energy technologies such as batteries and catalysts,<sup>13–15</sup> although such a design approach has yet to be applied to the problem of photoinduced structural transformation.

In this Letter, we demonstrate the potential of applying a high-throughput simulation approach to the design of STF materials. Through such an approach, we have (i) discovered a broad set of novel materials for STF applications from large molecular structure databases, (ii) showed that in many cases, although unintuitive, there are straightforward chemical modifications to existing photoswitches that could lead to dramatic improvements in their key properties for STF, and (iii) developed new design principles that can be extracted from our high-throughput screening.

Our screening platform consists of two phases. In the first phase, the program reads molecules from databases and uses classical potentials to search for isomerization patterns associated with photoactive bonds or groups, such as the N=N diazene bond. In the second phase, ab initio calculations are carried out to compute key STF properties such as the isomerization enthalpy for each of the isomerization patterns discovered in phase 1. Both phases are coded with JAVA to ensure cross-platform compatibility while maintaining reasonable speed and efficiency. In our first application of this approach, we limit our screening to the nitrogen double bond and molecules that only contain the elements C, H, O, N, and S, and we focus on screening for materials with high-energy storage ( $\Delta H$ ) and suitable absorption onset. Broader materials sets and other STF properties will be included in the further development of our platform.

The first phase must strike a balance between covering a wide range of possible photoswitched states while keeping the number of calculations reasonable (i.e., hundreds or thousands of full optimization runs per molecule). During this phase, we locate possible metastable states of each molecule by forcing the molecular structures to rotate around the N=N bond with two types of rotational degrees of freedom. As shown in Figure 1, one subgroup of the molecule is rotated around the N=N bond with a step size of  $5^\circ$ . During each of these steps, this subgroup also undergoes an in-plane rotation of up to  $45^\circ$  both toward and away from the N=N bond. This secondary rotational degree of freedom is also explored in  $5^\circ$  increments. The structure of the full molecule except the bond angles and dihedral angles associated with the N=N bond is relaxed during each exploration step using the REAX force field<sup>16</sup> as implemented in LAMMPS.<sup>17</sup> We record the relaxed structure as a candidate metastable structure if the energy difference between it and the initial structure is more than 0.5 eV (Supporting Information S1).

In the second phase, VASP<sup>18,19</sup> is used to relax the positions of all atoms until the forces acting on the ions are smaller than 0.01 eV/Å. The periodic box is set such that 10 Å of vacuum space is present in all three directions. All energies are calculated using density functional theory (DFT) with the exchange-correlation energy of Perdew–Burke–Ernzerhof<sup>20</sup> (PBE). Once the structure is relaxed, we evaluate the isomerization enthalpy ( $\Delta H$ ) by comparing the metastable state enthalpy with the enthalpy of the ground state configuration. We note that in the present work we considered only a relatively simple structural phase space (i.e., rotation of two subgroups around a given bond). From the standpoint of

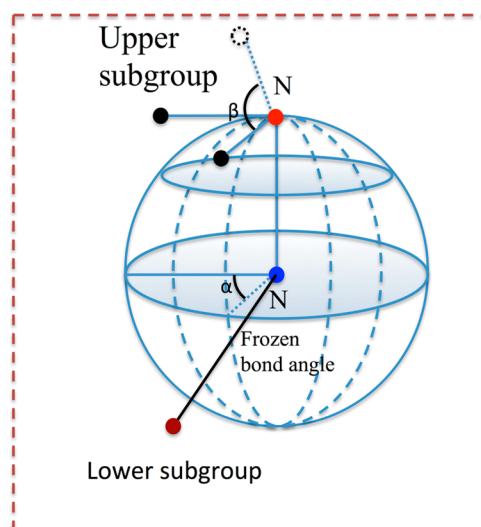


**Figure 1.** Rotational operation applied to each of the molecules during the screening step. The bond between the N atom and the lower subgroup is kept frozen at all time. The upper subgroup is first rotated around the N=N bond for  $\alpha^\circ$ , and then rotated toward or away from the N=N bond for  $\beta^\circ$ . The N=N is kept aligned with the Z-axis.

STF, this captures the classes of molecules that undergo strain upon photo excitation (e.g., azobenzene, stilbene), but not ones that break and reform covalent bonds reversibly, such as in the case of norbornadiene/quadracyclane. Nonetheless, the framework we have developed is quite general and can be easily extended to explore other regions of phase space; for instance, cutting the molecule at a random bond followed by the same approach of subgroup rotations as employed here, would lead to the discovery of STF in the bond breaking class of materials.

Figure 2 shows results for 919 isomerization patterns of 430 different molecules identified from the Cambridge Structural database (CSD) library. We have plotted our computed  $\Delta H$  and gaps ( $E_g$ ) between the highest occupied molecular orbital (HOMO) and the lowest unoccupied molecular orbital (LUMO). Note that for any given molecule there may be multiple metastable structures, which is why the number of isomerization patterns is greater than the number of molecules. As can be seen from Figure 2, the correlation between the two quantities  $\Delta H$  and  $E_g$  is quite weak. Most of the results lie in the square region bounded by  $0.0 \text{ eV} < \Delta H < 0.9$  and  $2.0 \text{ eV} < E_g < 3.5 \text{ eV}$ . Interestingly, even within this limited set of initial screening candidates, we find that 35% of the isomerization patterns possess a  $\Delta H > 0.6 \text{ eV}$ , the value for the case of azobenzene, which is a material that even in its unmodified form has been proposed as a STF.<sup>1</sup>

In order to assess which materials would make good solar thermal fuels, we need to revisit the criteria mentioned earlier. For the STF to absorb sunlight in the visible part of the spectrum, its  $E_g$  should be less than 3.0 eV. Considering that we used the GGA functional, we expect the HOMO–LUMO gaps to be underestimated in our calculations. Taking the difference between our calculated and experimentally measured gaps for azobenzene (1.9 eV in GGA vs 2.8 eV in experiment) as a rough guide, we can use a HOMO–LUMO gap of 2.1 eV as an initial condition for screening STF candidates (Supporting Information S2).

As can be seen in Figure 2b, which shows the total number of candidates as a function of their  $E_g$ , about 40% (372) of the isomerization patterns have  $E_g < 2.1 \text{ eV}$ . Figure 2c shows the

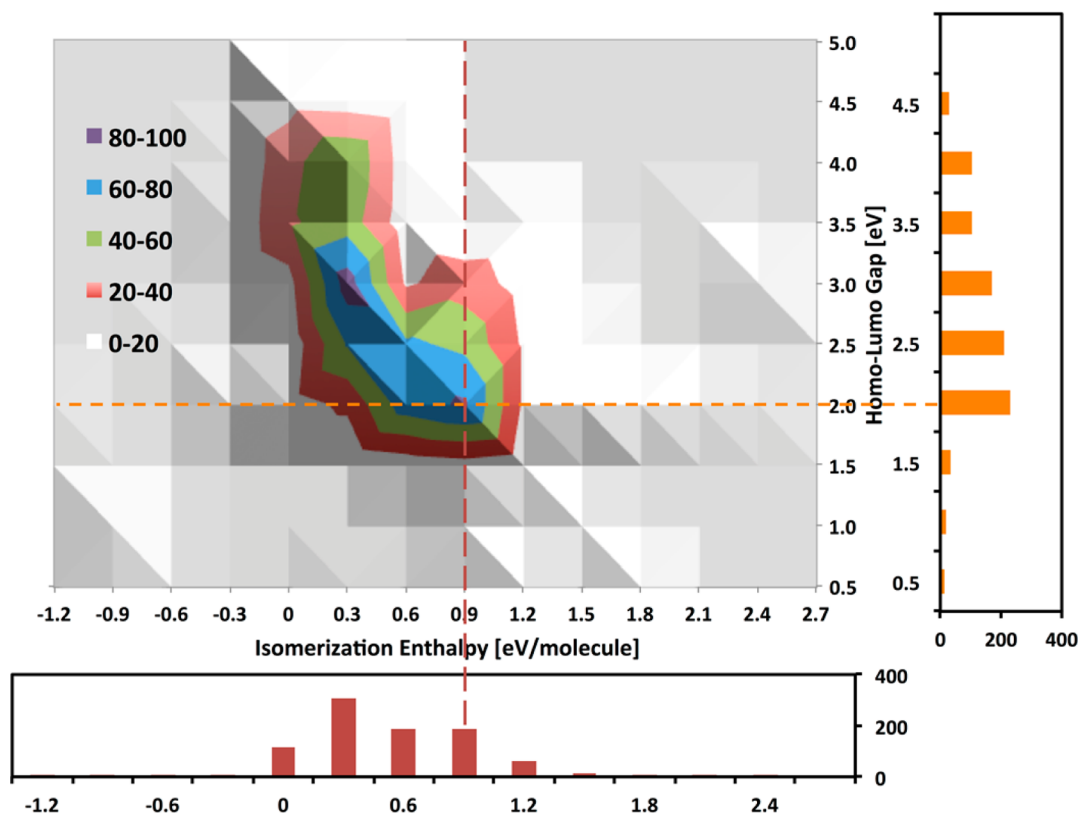


**Figure 2.** Number of isomerization patterns discovered, plotted against  $\Delta H$  and  $E_g$  at the trans state. (a) Two-dimensional plot of the number of isomerization patterns with respect to both  $\Delta H$  and  $E_g$ , colors correspond to number of patterns within a certain range of  $\Delta H$  and  $E_g$  are shown in the legend. (b,c) Projected number of patterns onto either  $\Delta H$  or  $E_g$ . Vertical and horizontal lines corresponds to the  $\Delta H > 0.9$  eV and  $E_g < 2.1$  eV screening conditions, respectively.

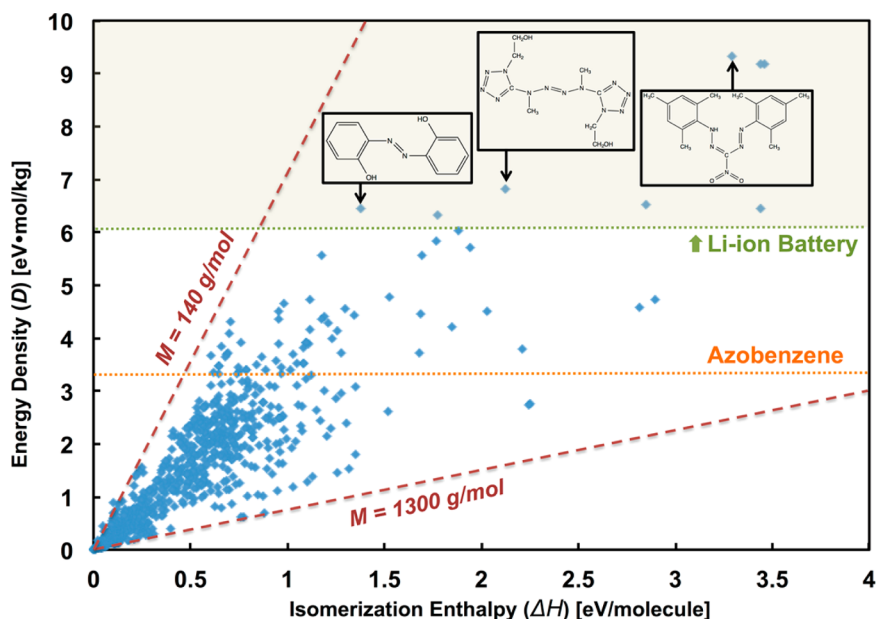


**Figure 3.** Energy density versus isomerization enthalpy for STF materials screened in this work. Chemical structures of three high gravimetric energy density materials are also shown. For comparison, the energy density of free azobenzene is shown with dotted orange line. The dotted green line corresponds to the lower bound of energy density for Li-ion batteries. The two red dashed lines show the upper and lower bounds of the molecular weight of the materials we have screened.

number of candidates versus their computed  $\Delta H$ . Roughly 10% (98) of the isomerization patterns have  $\Delta H > 0.9$  eV, which represents a 50% increase over azobenzene. About 6.7%, or 62 isomerization patterns, satisfy both the  $E_g < 2.1$  eV and  $\Delta H >$

0.9 eV screening conditions (see Supporting Information S3 for a complete list). Statistically, if  $\Delta H$  and  $E_g$  were completely independent, the ratio of isomerization patterns satisfying both conditions would be the product of 40 and 10%, which is about

4%. The slightly higher ratio of 6.7% we obtain from our results shows there is correlation between  $\Delta H$  and  $E_g$ . In fact, one can visually see from Figure 2a that there are two peaks on this plot. The upper left peak corresponds to molecules with high  $E_g$  and low  $\Delta H$ , which is not interesting to us; on the other hand, the lower right peak corresponds to molecules with both high  $\Delta H$  and low  $E_g$ , which is well suited for STF applications.

The gravimetric energy density, or the amount of energy stored per kilogram, is another important metric for STF. A large molecule with a high  $\Delta H$  may have a low energy density due to its heavy weight. We have calculated the energy density of each isomerization pattern by dividing  $\Delta H$  by the molecular weight ( $M$ , in units of kg/mol), giving energy densities as eV·mol/kg, or roughly 0.1 MJ/kg. In Figure 3, we plot the energy densities for all the isomerization patterns we have found. The specific energy density of current lithium ion batteries (>0.6 MJ/kg) is shown for comparison.<sup>21</sup> The slopes of the lines on this plot are inversely proportional to the weight of the molecules ( $M$ ) associated with the points on the line. The two red lines correspond to the upper and lower bounds of the weights of the molecules in this particular screening set. The fact that the data scatter evenly between the two dashed red lines suggests that  $\Delta H$  and  $M$  have little correlation with each other.

These results demonstrate that, even starting with a considerably restricted set of molecules, our high-throughput approach can identify a collection of high-performance materials that have not previously been considered for STF applications. Further, the identified materials are predicted to provide energy densities as high as norbornadiene (0.96 MJ/kg),<sup>22</sup> which is the highest energy density STF experimentally realized to date.

In addition to the use of such a screening approach to search directly for high performance solar thermal fuel materials, we are also interested in gaining a deeper understanding of the physical mechanisms that lead to high  $\Delta H$  materials with the aim of developing general design principles for STF. Toward this end, we have carried out a structural analysis of our data and identified three distinct classes of molecular attributes.

The first group of molecules has at least one hydroxyl group on the molecule that is capable of forming a hydrogen bond with the N=N double bond at the trans state (Figure 4a,b). This extra hydrogen bond stabilizes the trans structure and increases the enthalpy difference between the trans and cis states. It is worth noting that independent of this study this principle has already been shown to be useful for the development of STF<sup>9</sup> although here it is demonstrated more broadly across a large set of structures. The second group of molecules possess a N-H group that is capable of forming hydrogen bonds with the N=N double bond at the trans state (Figure 4c,d). This may at first appear similar to the hydroxyl group effect; however, the N-H group is different from the O-H group as the N-H group is capable of forming two extra bonds instead of one. Therefore, the N-H group can be a structure linker rather than just an end group (as demonstrated in Figure 4c), which increases the variety of molecular structures into which it can be incorporated. In the third group of molecules, the structures possess multiple aromatic rings, forming effectively a small cluster. The  $\pi$ - $\pi$  stacking effects between the phenyl rings within the molecule can lead to a stabilization of the trans structure. When the molecule is transformed to its cis configuration, the stacking is interrupted and the free energy increased (Figure 4e,f). One may

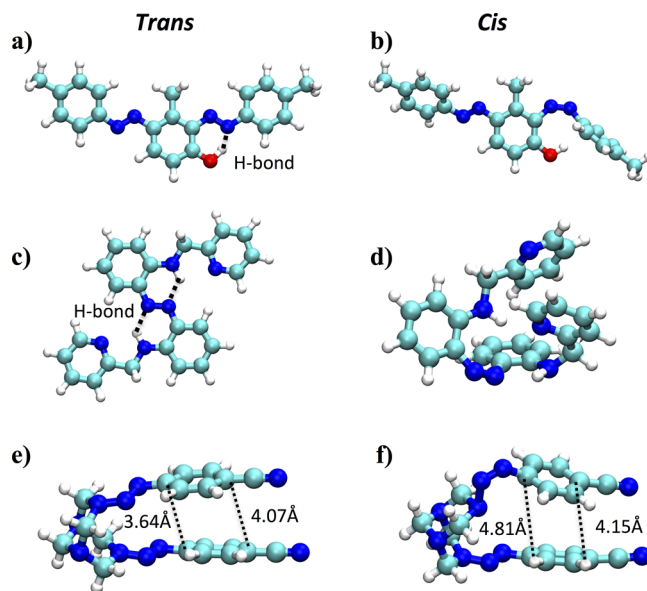


**Figure 4.** Representatives of three groups of high  $\Delta H$  STF candidate materials summarized from our results. (a,b) Correspond to molecules capable of forming hydrogen bonds through the hydroxyl group. (c,d) Correspond to molecules capable of forming hydrogen bonds through a secondary amine group. (e,f) Correspond to molecules capable of forming  $\pi$ - $\pi$  stacking between end groups. Dashed lines in the first two trans configurations (a,c) illustrate hydrogen bonds. Dashed black lines in a) and c) highlight the hydrogen bonds that are broken during the *trans* to *cis* isomerization (not all of the molecules we found can be defined as “*cis*” or “*trans*”. However, for all the molecules we show in this manuscript, the *trans*-*cis* notation works well).

reasonably assume that the  $\pi$ - $\pi$  stacking effect can be increased or decreased by adding or removing rings from the end group and that this effect may therefore provide an extra degree of freedom to control the  $\Delta H$ . One benefit of using this strategy to control the  $\Delta H$  is that the stacking effect can be directly controlled by the number of conjugated rings that are interacting with each other. Therefore, by changing the number of rings or the separation between them, one can freely control the strength of the  $\pi$ - $\pi$  stacking and therefore the  $\Delta H$ .

In summary, we have developed a high-throughput ab initio simulation platform for discovering novel STF materials. Using this platform, we have identified a set of possible candidates with high energy-storage capacity from the CSD library. One advantage of our approach is that all the materials we identified are from a public database where most of the molecules have already been experimentally synthesized and characterized. With mature production protocols in hand, experimental verification of these candidate materials can jump immediately to the stage of quantification of energy storage density. In addition, the materials and design principles discovered in this work could be used in parallel with other design strategies such as templating,<sup>10</sup> which can further expand the chemical phase space for STF materials. We note that the results presented here are from screening only a small subset of molecules in the CSD, that is, containing earth-abundant elements and the N=N subgroup. We believe that the extension of this approach to broader classes of materials will result in further candidate chemistries, and beyond STF applications the materials discovered with such an approach have the potential to impact a range of other photochromism-related research fields, such as molecular switches.<sup>23</sup>

## ■ ASSOCIATED CONTENT

### Supporting Information

SI includes the atomic configuration and visual comparison of the 62 candidate isomerization patterns. This material is available free of charge at <http://pubs.acs.org>. The library of all identified STF candidates can be found free online at <http://zeppola.mit.edu>. This material is available free of charge via the Internet at <http://pubs.acs.org>.

## ■ AUTHOR INFORMATION

### Corresponding Authors

\*E-mail: [yunl@mit.edu](mailto:yunl@mit.edu).

\*E-mail: [jcg@mit.edu](mailto:jcg@mit.edu).

### Funding

This work is supported by the Advanced Research Projects Agency-Energy (ARPA-E), US Department of Energy, under award number DE-AR0000180.

### Notes

The authors declare no competing financial interest.

## ■ ACKNOWLEDGMENTS

The *ab initio* calculations are carried out on HOPPER from NERSC and STAMPEDE from XSEDE. The authors acknowledge Prof. Kolpak and Prof. Ceder from MIT for helpful discussions.

## ■ REFERENCES

- (1) Jones, I. G.; Chiang, S.-H.; Xuan, P. T. *J. Photochem.* **1979**, *10*, 1–18.
- (2) Boese, R.; Cammack, J. K.; Matzger, A. J.; Pflug, K.; Tolman, W. B.; Vollhardt, K. P. C.; Weidman, T. W. *J. Am. Chem. Soc.* **1997**, *119*, 6757–6773.
- (3) Alexander, D. D.; Vladimir, A. B.; Chernouvanov, V. A. *Russ. Chem. Rev.* **2002**, *71*, 917–927.
- (4) Gur, I.; Sawyer, K.; Prasher, R. *Science* **2012**, *335*, 1454–1455.
- (5) Olmsted III, J.; Lawrence, J.; Yee, G. G. *Sol. Energy* **1983**, *30*, 271–274.
- (6) Durgun, E.; Grossman, J. C. *J. Phys. Chem. Lett.* **2013**, *4*, 854–860.
- (7) Moth-Poulsen, K.; Coso, D.; Borjesson, K.; Vinokurov, N.; Meier, S. K.; Majumdar, A.; Vollhardt, K. P. C.; Segalman, R. A. *Energy Environ. Sci.* **2012**, *5*, 8534–8537.
- (8) Hou, Z.; Nguyen, S. C.; Lomont, J. P.; Harris, C. B.; Vinokurov, N.; Vollhardt, K. P. C. *Phys. Chem. Chem. Phys.* **2013**, *15*, 7466–7469.
- (9) Kolpak, A. M.; Grossman, J. C. *Nano Lett.* **2011**, *11*, 3156–3162.
- (10) Kolpak, A. M.; Grossman, J. C. *J. Chem. Phys.* **2013**, *138*, 034303.
- (11) Kucharski, T. J.; Ferralis, N.; Kolpak, A. M.; Zheng, J. O.; Nocera, D. G.; Grossman, J. C. *Nat. Chem.* **2014**, *6*, 441–447.
- (12) Committee on Integrated Computational Materials Engineering, N. R. C. *Integrated Computational Materials Engineering: A Transformational Discipline for Improved Competitiveness and National Security*; The National Academy Press: Washington, DC, 2008; p 152.
- (13) Norskov, J. K.; Bligaard, T.; Rossmeyl, J.; Christensen, C. H. *Nat. Chem.* **2009**, *1*, 37–46.
- (14) Jain, A.; Hautier, G.; Moore, C. J.; Ping Ong, S.; Fischer, C. C.; Mueller, T.; Persson, K. A.; Ceder, G. *Comput. Mater. Sci.* **2011**, *50*, 2295–2310.
- (15) Curtarolo, S.; Setyawan, W.; Hart, G. L. W.; Jahnatek, M.; Chepulskii, R. V.; Taylor, R. H.; Wang, S.; Xue, J.; Yang, K.; Levy, O.; Mehl, M. J.; Stokes, H. T.; Demchenko, D. O.; Morgan, D. *Comput. Mater. Sci.* **2012**, *58*, 218–226.
- (16) van Duin, A. C. T.; Dasgupta, S.; Lorant, F.; Goddard, W. A. *J. Phys. Chem. A* **2001**, *105*, 9396–9409.
- (17) Plimpton, S. J. *Comput. Phys.* **1995**, *117*, 1–19.

- (18) Kresse, G.; Furthmüller, J. *Phys. Rev. B* **1996**, *54*, 11169–11186.
- (19) Kresse, G.; Joubert, D. *Phys. Rev. B* **1999**, *59*, 1758–1775.
- (20) Perdew, J. P.; Burke, K.; Ernzerhof, M. *Phys. Rev. Lett.* **1996**, *77*, 3865–3868.
- (21) Wagner, R.; Preschitschek, N.; Passerini, S.; Leker, J.; Winter, M. *J. Appl. Electrochem.* **2013**, *43*, 481–496.
- (22) An, X.-w.; Xie, Y.-d. *Thermochim. Acta* **1993**, *220*, 17–25.
- (23) Natali, M.; Giordani, S. *Chem. Soc. Rev.* **2012**, *41*, 4010–4029.